THE ASTROPHYSICAL JOURNAL, 472:25–33, 1996 November 20

THE COMPATIBILITY OF FRIEDMANN COSMOLOGICAL MODELS WITH OBSERVED PROPERTIES OF GAMMA-RAY BURSTS AND A LARGE HUBBLE CONSTANT

JOHN M. HORACK,[1] THOMAS M. KOSHUT,[2] ROBERT S. MALLOZZI,[3]
A. GORDON EMSLIE,[3] AND CHARLES A. MEEGAN[1]
Received 1995 December 4; accepted 1996 June 5

ABSTRACT

The distance scale to cosmic gamma-ray bursts (GRBs) is still uncertain by many orders of magnitude; however, one viable scenario places GRBs at cosmological distances, thereby permitting them to be used as tracers of the cosmological expansion over a significant range of redshifts z. Also, several recent measurements of the Hubble constant H_0 appearing in the referred literature report values of 70–80 km s^{-1} Mpc^{-1}. Although there is significant debate regarding these measurements, we proceed here under the assumption that they are evidence of a large value for H_0. This is done in order to investigate the additional constraints on cosmological models that can be obtained under this hypothesis when combined with the age of the universe and the brightness distribution of cosmological gamma-ray bursts.

We show that the range of cosmological models that can be consistent with the GRB brightness distribution, a Hubble constant of 70–80 km s^{-1} Mpc^{-1}, and a minimum age of the universe of 13–15 Gyr is constrained significantly, largely independent of a wide range of assumptions regarding the evolutionary nature of the burst population. Low-density, $\Lambda > 0$ cosmological models with deceleration parameter in the range $-1 < q_0 < 0$ and density parameter σ_0 in the range $\approx$0.10–0.25 ($\Omega_0 \approx$ 0.2–0.5) are strongly favored.

Subject headings: cosmology: theory — distance scale — gamma rays: bursts

1. INTRODUCTION

Gamma-ray bursts (GRBs) exhibit an angular distribution that is consistent with isotropy, yet their brightness distribution indicates that the burst sources are either inhomogeneously distributed, embedded in a non-Euclidean space, or both (Meegan et al. 1992). Since no known Galactic objects possess both these properties, and since cosmological models explain naturally both the angular isotropy and the deviation from Euclidean homogeneity, the hypothesis that gamma-ray bursts are cosmological (Paczyński 1991) has gained significant acceptance.

Several studies have addressed the form of the cosmological GRB brightness distribution. Early works (e.g., Mao & Paczyński 1992; Fenimore et al. 1993; Wickramasinghe et al. 1993) demonstrated that the brightness distribution observed with the Burst and Transient Source Experiment (BATSE) is consistent with nonevolving, standard-candle sources embedded in a spatially flat ($k = 0$) universe with critical density ($\Omega_0/2 = \sigma_0 = 0.5$) and zero cosmological constant Λ, and that these bursts are visible to limiting redshifts of order unity. Later analyses (e.g., Emslie & Horack 1994) showed that in models in which $\Lambda = 0$, the limiting redshift is largely insensitive to the value of q_0; however larger limiting redshifts are consistent with the BATSE data for accelerating ($q_0 < 0$) models with nonzero Λ. Models incorporating burst source evolution (e.g., Horack, Emslie, & Hartmann 1995; Rutledge, Hui, & Lewin 1995; Meszáros & Meszáros 1995) demonstrated that higher limiting redshifts are possible for burst populations in which the comoving rate density of bursts increases with redshift. Most of the emphasis in these works is on "standard" cosmological models in which the cosmological constant is assumed to be exactly zero.

Interest in models with $\Lambda > 0$ has been renewed, however, by a recent series of measurements of the Hubble constant H_0 in the range 70–80 km s^{-1} Mpc^{-1}, obtained through the *Hubble Space Telescope* (*HST*) and from ground-based measurements. For example, Freedman et al. (1994), observing the galaxy M100 using *HST*, report a value of $H_0 = 80 \pm 17$ km s^{-1} Mpc^{-1}. Pierce et al. (1994) obtain a larger value of $H_0 = 87 \pm 7$ km s^{-1} Mpc^{-1} through a study of NGC 4571 utilizing the Canada-France-Hawaii Telescope on Mauna Kea. Observations by Tanvir et al. (1995) of M96 with *HST* have resulted in a value of 69 ± 8 km s^{-1} Mpc^{-1}. If correct, when combined with a minimum age of the universe of 13–15 billion years, these measurements *require* (e.g., Leonard & Lake 1995) that $\Lambda > 0$.

The value of H_0 in general, and the previous measurements (as well as others) in particular, is currently the subject of debate. It is not certain that H_0 is in the range reported by the aforementioned authors, and indeed some measurements (e.g., Sandage et al. 1996) yield H_0 values significantly less than 70 km s^{-1} Mpc^{-1}. Our purpose here is not to provide a critique or assessment of the validity of the many H_0 measurements.

Instead, we proceed under the assumption that the aforementioned measurements, as well as others, are indications of a large value for H_0, without significant consideration of the arguments for or against either a particular range of values for H_0 or a particular published analysis. Under this assumption, the combination of a large value for H_0 with the independently obtained brightness distribution of gamma-ray bursts yields constraints that are unavailable from either observation alone.

We begin with a brief discussion of the mathematics necessary to address this problem. This section is followed

[1] Space Science Laboratory, NASA/MSFC, ES-84, Huntsville, AL 35812.
[2] Universities Space Research Association, Mail Stop ES-84, Huntsville, AL 35812.
[3] Department of Physics, University of Alabama in Huntsville, AL 35899.

by analyses of the brightness distribution of the BATSE 3B (Meegan et al. 1996) catalog of bursts. Here we obtain χ^2 probabilities from fits of the observed differential brightness distribution $N(P)$ to the distribution predicted by various cosmological models. The information obtained from these probabilities is then united with the (wholly independent) determinations of H_0 and the age of the universe to obtain a quantitative estimate of the cosmological model's ability to reliably reproduce data consistent with both sets of observations.

2. ANALYSIS

2.1. *Hubble Constant and Universe Age*

We examine Friedmann dust cosmologies that admit a nonzero cosmological constant Λ. For such models, the age of the universe τ_0 can be written as

$$y(\sigma_0, q_0) \equiv \tau_0 H_0 = \int_0^\infty \frac{(1+z')^{-1}\,dz'}{\sqrt{2\sigma_0(1+z')^3 + (1+q_0-3\sigma_0)(1+z')^2 + (\sigma_0 - q_0)}}, \quad (1)$$

where σ_0 is the density parameter and q_0 is the deceleration parameter. For the Einstein–de Sitter model ($\Lambda = 0$, $\sigma_0 = q_0 = 0.5$), this integral is readily evaluated, yielding $y = \frac{2}{3}$.

Given a reliable lower limit to τ_0 (obtained, for example, from detailed stellar evolution calculations), we can use equation (1) to obtain the region in the (σ_0, q_0) plane that is consistent with both the estimated age of the universe τ_0 and current estimates of H_0.

To begin the analysis, we must first select an acceptable set of H_0 measurements that are commensurate with the goal of the investigation, namely, to explore the implications of a large Hubble constant in conjunction with the brightness distribution of cosmological gamma-ray bursts. For the purposes of the analysis, we must assume also that these measurements are an indication that H_0 may indeed be large and that its value is well estimated by the measurements in question. To this end, we focus specifically on the family of Hubble constant measurements obtained through recent *HST* observations of the Virgo Cluster galaxy M100 (Freedman et al. 1994; Mould et al. 1995). These are summarized in Table 1.

The average of the quantities in Table 1 is 78 km s^{-1} Mpc^{-1}. We adopt this as our "best-estimate" value for H_0. To estimate the uncertainty in this value, we have performed a computation of the full covariance matrix for these seven measurements. This accounts for the common sources of error; the distance to M100, found in all methods, and the distance to the Virgo Cluster, found in all except the Type Ia SN standard-candle method.

TABLE 1

H_0 VALUES FROM M100 OBSERVATIONS

Value (km s^{-1} Mpc^{-1})	Method	Reference
80 ± 17	Recession velocity	1
81 ± 11	Recession velocity	2
73 ± 11	Type II SN distance	2
84 ± 16	Surface brightness fluctuation	2
76 ± 10	Elliptical galaxy velocity dispersion	2
82 ± 11	Tully-Fisher relation	2
71 ± 10	Type Ia SN standard candle	2

REFERENCES.—(1) Freedman et al. 1994; (2) Mould et al. 1995.

We obtain a value of $H_0 = 78 \pm 9$ km s^{-1} Mpc^{-1}. Because of the sources of uncertainty common to the methods, the combination of a number of different measurements has only minimal impact on the reduction of the size of the overall uncertainty. This value is consistent with other recent singular measurements of H_0, for example, that of Whitmore et al. (1995) (78 ± 11 km s^{-1} Mpc^{-1}) from observations of M87 in the Coma Cluster, and it is more conservative in both magnitude and error estimation than the Pierce et al. (1994) measurement of 87 ± 7 km s^{-1} Mpc^{-1} obtained from observations of NGC 4571 in the Virgo Cluster.

A similar set of measurements is required for the age of the universe. We utilize the recent age measurements of Bolte & Hogan (1995) ($\tau_0 = 15.8 \pm 2.1$ Gyr), Chaboyer (1994) ($\tau_0 = 15.5 \pm 4$ Gyr), and van den Bergh (1991) ($\tau_0 = 16.5 \pm 2$ Gyr). These are averaged to determine a best-estimate value for τ_0 of 15.9 Gyr. The full covariance matrix is employed again to determine a measure of the uncertainty in our best-estimate value of τ_0. However, in addition to common uncertainties such as the RR Lyrae distance scale, there are others, such as common stellar evolution physics incorporated into numerical simulations, that are more difficult to quantify. Therefore, to avoid obfuscating the main intent of the paper with details of uncertainty calculation and estimation, we make the simplifying assumption that the off-diagonal terms in the τ_0 covariance matrix are comparable in size to the typical diagonal terms. This assumption, although somewhat arbitrary, is quantitatively more conservative than the covariance matrix calculated for the H_0 case, and it yields a result of 15.9 ± 2.3 Gyr.

This estimate of the age of the universe is consistent with other recent estimates, for example, the Sommer-Larsen (1996) value of 17 ± 2 Gyr. Chaboyer (1995) has also estimated the age of the universe, employing a standard stellar evolution model (as well as many modifications) with both the Layden et al. (1995) and Walker (1992) RR Lyrae distance scales. The Chaboyer (1995) standard values obtained with each RR Lyrae distance scale are within 1 σ of the best-estimate value of τ_0 computed above.

Having obtained best-estimate values for H_0 and τ_0, these are then combined to determine a measured value for the dimensionless product $y_0 = \tau_0 H_0$, resulting in

$$y_0 = 1.27 \pm 0.23\,. \quad (2)$$

Figure 1 is a contour plot of $y(\sigma_0, q_0)$ as evaluated from equation (1). For reference, spatially flat [$(3\sigma_0 - q_0 - 1) = 0$] models are located along the dashed line labeled $k = 0$. Models with zero cosmological constant are located on the dot-dashed line labeled $\Lambda = 0$. The standard Einstein–de Sitter model, which possesses both the above properties, is located at the intersection of the two lines at which $\sigma_0 = q_0 = 0.5$. The contour for the best-estimate value (2) is also explicitly shown in the figure. We observe that the only cosmological models consistent with the value $y_0 \approx 1.27$ are accelerating ($q_0 < 0$). This result, which applies for all $y > 1$, is well known. What remains to be determined is whether the brightness distribution of gamma-ray bursts observed by BATSE is also consistent with any of the cosmological models that correspond to the measured value of y_0.

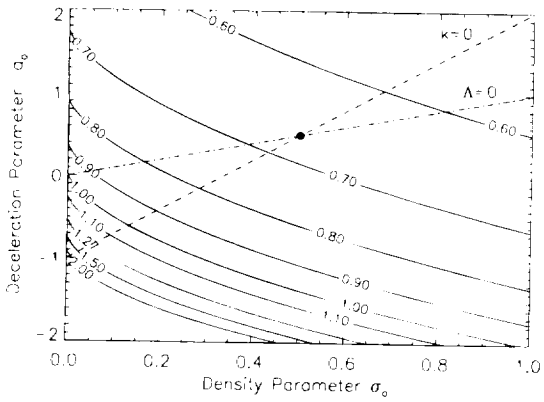

FIG. 1.—Values of $y(\sigma_0, q_0)$ as determined from equation (1). Spatially flat ($k = 0$) models are located on the dashed line, and $\Lambda = 0$ models are located on the dot-dashed line.

2.2. *The GRB Peak Flux Distribution*

We measure the brightness P of a gamma-ray burst in terms of its peak flux (photons cm^{-2} s^{-1}), measured over a time interval of 0.256 s in the energy range 50–300 keV. For a given GRB located at redshift z, this brightness can be written

$$P = \frac{L(z)(1+z)}{4\pi d_l^2}, \tag{3}$$

where d_l is the luminosity distance, $d_l = S_0 r(z)(1+z)$, S_0 is the local value of the scale factor, and $r(z)$ is the radial coordinate of the burst at redshift z. The functional form of $r(z)$ depends on the specific cosmological model in question. The quantity $L(z)$ (photons s^{-1}) is the portion of the bolometric source luminosity that is accessible to the finite energy bandwidth of the detector. It can be written as

$$L(z) = \int_{E_1(1+z)}^{E_2(1+z)} \phi(E')dE' . \tag{4}$$

Here E_1 and E_2 are the lower and upper limits to the energy visible by the detector (for BATSE 50 and 300 keV, respectively). Employing a power-law spectral form for the gamma-ray bursts' luminosity distribution (photons s^{-1} keV^{-1}),

$$\phi(E) = A_0 E^{-\alpha}, \tag{5}$$

with $\alpha > 0$, we obtain

$$P = \frac{L_0(1+z)^{2-\alpha}}{4\pi d_l^2}, \tag{6}$$

with $L_0 = \int_{E_1}^{E_2} \phi(E)dE$.

Figure 2 contains both the integral $\mathcal{N}(>P)$ and differential $N(P)$ brightness distributions from the third BATSE gamma-ray burst catalog (Meegan et al. 1996). The lines labeled $-3/2$ and $-5/2$ in the integral and differential plots, respectively, indicate the shape of the brightness distribution expected from a homogeneous population of bursts in Euclidean space. The deviation of the data from this relation is apparent, occurring nearly an order of magnitude above the instrumental threshold.

This deviation from Euclidean homogeneity may be due, at least in part, to cosmological effects. For a population of monoluminous gamma-ray bursts distributed with comoving rate density prescribed by $n_c(z)$, the observed rate of bursts $\mathcal{N}(>P')$ with brightness larger than some value P' can be written

$$\mathcal{N}(>P') \propto \int_0^{z(P')} \frac{n_c(z)}{(1+z)} r^2(z) f(z) dz , \tag{7}$$

where

$$f(z) = \frac{1}{\sqrt{2\sigma_0(1+z)^3 + (1+q_0-3\sigma_0)(1+z)^2 + (\sigma_0 - q_0)}} . \tag{8}$$

The factor of $(1+z)$ in the denominator of equation (7) accounts for the fact that one is measuring a *rate* of burst occurrence, and the time between bursts at large redshifts will itself be cosmologically dilated by a factor of $(1+z)$. The quantity $z(P')$ is the redshift value that satisfies equation 6 for a specified brightness P'.

The differential brightness distribution $N(P)$ is defined

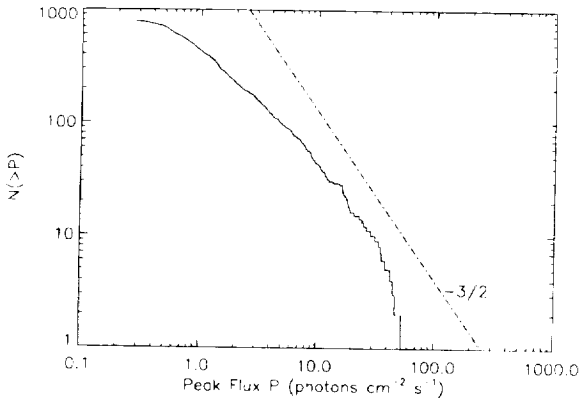

FIG. 2a

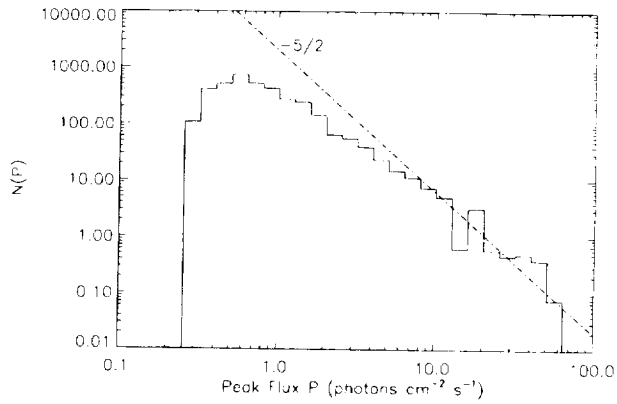

FIG. 2b

FIG. 2.—(*a*) Integral and (*b*) differential brightness distributions for gamma-ray bursts in the third BATSE gamma-ray burst catalog (Meegan et al. 1996). The units of brightness are photons cm^{-2} s^{-1} in the interval 50–300 keV computed on a 0.256 s timescale. The broken lines marked $-3/2$ and $-5/2$ in the integral and differential plots, respectively, indicate the shape expected for a homogeneous distribution of sources in Euclidean space.

such that $N(P)dP$ is the rate of observed bursts with brightnesses between P and $P + dP$:

$$N(P) = -\frac{d}{dP}\mathcal{N}(>P) . \quad (9)$$

It is straightforward to construct a model differential brightness distribution $N_M(P)$ from a set of cosmological parameters (σ_0, q_0), spectral index α, burst comoving rate density function $n_c(z)$, and limiting redshift $z_{0.5}$. These five quantities constitute a "cosmological model." In the work that follows, we shall parameterize the comoving rate density as $n_c(z) \propto (1 + z)^\beta$, where β is a free parameter. A value of $\beta = 0$ corresponds, therefore, to a constant (no evolution) comoving rate density. The use of the limiting redshift as a parameter in the model assigns a particular value of z to a particular peak flux P. This is equivalent to attribution of a specific luminosity L (photons s^{-1}) to the gamma-ray bursts. In construction of burst models, the parameterization of the burst luminosity can be done either by assigning a value directly to the bursts (e.g., Fenimore et al. 1993), or through the use of z_P (e.g., Horack, Mallozzi, & Koshut 1996b).

The resulting model brightness distribution $N_M(P)$ can be tested against the observed brightness distribution in Figure 2*b* using the χ^2 test. One thereby obtains both a value for the reduced χ^2 statistic and a probability $P(>\chi^2)$ that a random sample taken from the model would result in a distribution of equal or greater disparity than the observed data. Low values of $P(>\chi^2)$, therefore, indicate that the model is unlikely to be the correct one, as it fails to reproduce a model distribution $N_M(P)$ similar to the observed $N(P)$.

Figure 3 shows a contour plot of $P(>\chi^2)$ in the (σ_0, q_0) plane. In generating this example, we have assumed a constant comoving rate density of bursts $n_c(z)$ and a photon spectral index $\alpha = 2$, and that bursts that are located at a redshift of unity produce a peak flux of 0.5 photons cm^{-2} s^{-1} $(z_{0.5} = 1)$.

The compliance of the brightness distribution with all decelerating $(q_0 > 0)$ cosmological models noted in the introduction is also demonstrated in Figure 3. For this spectral index, comoving rate density, and limiting redshift, the capability of rejecting models on the basis of $P(>\chi^2)$ is largely insensitive to the value of both σ_0 and q_0 for decelerating models. As $P(>\chi^2)$ exceeds 0.5 for all these models, the null hypothesis cannot be rejected.

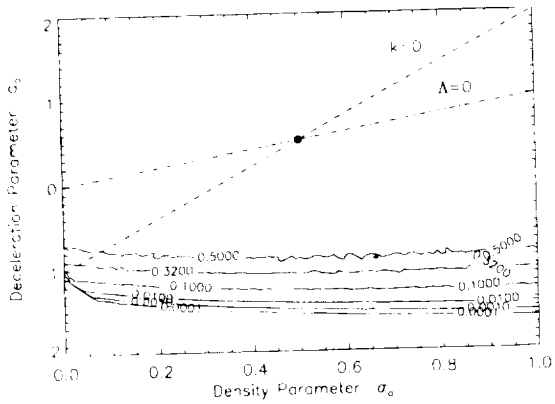

FIG. 3.—Contours of $P(>\chi^2)$ in the (σ_0, q_0) plane for a cosmological model with constant comoving rate density $n_c(z)$, power-law burst spectral index $\alpha = 2$, and limiting redshift of $z_{0.5} = 1$. These probabilities are obtained by application of the χ^2 test between the differential brightness distribution predicted by the model and the distribution obtained by BATSE (Fig. 2*b*).

3. COMBINING THE MEASUREMENTS

3.1. *Probabilities for* $y = \tau_0 H_0$

In Figure 1, we presented the computed values of $y(\sigma_0, q_0)$ found by evaluating the integral in equation (1) for points in the (σ_0, q_0) plane. We noted also that given the observations of H_0 and estimates of the age of the universe, their product is measured to be $y_0 \pm \sigma_{y_0} = 1.27 \pm 0.23$. Assuming a (minimal information) Gaussian distribution for the measurement distribution variable y', it is straightforward to compute for each point in the (σ_0, q_0) plane a probability value

$$\mathcal{P}(|y' - y_0| > |y - y_0|) = \frac{2}{\sqrt{2\pi}} \int_{|y - y_0|/\sigma_y}^{\infty} e^{-y'^2/2} dy' = \mathrm{erfc}\left(\frac{|y - y_0|}{\sigma_{y_0}\sqrt{2}}\right) . \quad (10)$$

This value represents the probability that a measurement of the value of y' will be realized to be equally or more discrepant from the value y_0 than the calculated value $y(\sigma_0, q_0)$ that the model predicts. Points in the (σ_0, q_0) plane that yield very low probabilities $\mathcal{P}$ are unlikely to represent reality, as they predict a value y that is inconsistent with the measurement y_0 at a high level.

For example, we have seen that the integral in equation (1), when evaluated with $\sigma_0 = q_0 = 0.5$, is equal to 2/3, which is approximately 2.6 standard errors removed from the measured value of 1.27. Thus, the value of $\mathcal{P}$ assigned to this point in the plane is erfc $(2.6/2^{1/2}) \approx 9.32 \times 10^{-3}$. That the inconsistency between the measured value y_0 and the value predicted by the Einstein–de Sitter model is on the order of 3 σ has been noted in previous works (e.g., van den Bergh 1992), and it is one measure of the relative merit of both the value y_0 used here and its computed uncertainty.

3.2. *Combining with the GRB* χ^2 *Probabilities*

To this point, we have determined the goodness of fit between the BATSE gamma-ray burst brightness distribution and the distribution predicted by the cosmological model in question, as well as the goodness of fit between the measured value y_0 and the value $y(\sigma_0, q_0)$ predicted by the model. We would like to combine these two pieces of information in a way that treats both of them with equal importance and allows for the rejection of a particular cosmological model on the basis of its level of disagreement with either the brightness distribution or the measured value of y. The situation is analogous to the consideration of a Galactic geometric burst model that predicts both a brightness distribution (e.g., Hakkila et al. 1995) and values for the two angular distribution moments (e.g., Briggs et al. 1996) $\langle \cos\theta \rangle$ and $\langle \sin^2 b \rangle$.

By adopting the reasonable assumption that the measurements of $\tau_0 H_0$ obtained in part from observations carried out with the *Hubble Space Telescope* are independent of the measured brightness distribution of gamma-ray bursts obtained with BATSE on the *Compton Gamma Ray Observatory*, a joint probability P_j can be obtained for each

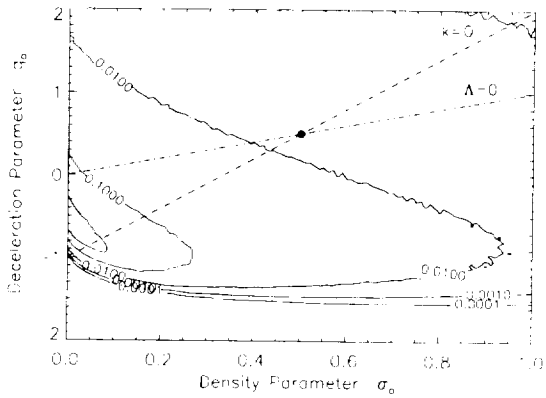

FIG. 4.—Joint probability contours P_j for the cosmological model used in Fig. 3. These data express the probability that a random sampling from the cosmological model would return *both* a χ^2 value more discrepant than the one obtained by comparing the model $N_M(P)$ to the BATSE distribution, and that a measurement of y would be obtained farther from $y_0 = 1.27 \pm 0.19$ than the value predicted by the model through equation (1). For this set of parameters, many high-density and most decelerating models can be ruled out with a high degree of confidence, as they predict values of y and/or a brightness distribution that are significantly in disagreement with observational data.

point in the (σ_0, q_0) plane by simply multiplying $P(>\chi^2)$ and $\mathscr{P}$, i.e.,

$$P_j = P(>\chi^2)\ \mathrm{erfc}\left(\frac{|y - y_0|}{\sigma_{y_0}\sqrt{2}}\right). \qquad (11)$$

The quantity P_j is the probability that a random sampling from the cosmological model in question would return *both* a χ^2 value more discrepant than the one obtained comparing the model to the BATSE brightness distribution *and* a measurement value y' that is farther from $y_0 = 1.27 \pm 0.23$ than the y calculated from equation (1).

We employ P_j as our statistic to assess a model's capability to reproduce observations of both the brightness distribution and value of y. As such, it is more demanding than either of the individual estimators $[P(>\chi^2)$ or $\mathscr{P}]$ alone. It is also a significantly stronger test for rejection than a global χ^2, computed as the sum of the χ^2 from the brightness distribution and the value $(y - y_0)^2/\sigma_y^2$, and it treats the measurement of y on equal footing with only one bin of the brightness distribution rather than the overall goodness of fit.

We stress that P_j is used here only to reject models. Models which yield very low values of P_j are unlikely to be the actual cosmological configuration found in nature, as they predict a brightness distribution and/or value of y that is significantly different from those observed. Conversely, models yielding large values of P_j cannot be rejected, as they reproduce both a brightness distribution and value of y consistent with observation. The value of P_j that one chooses as the threshold for rejection of a particular model is, of course, ultimately a scientific judgment. Figure 4 shows one example of $P_j(\sigma_0, q_0)$ for the same cosmological model employed in Figure 3.

4. RESULTS OF COMBINING MEASUREMENTS

Figures 5*a*–5*d* show the results of combining these two probabilities for a variety of assumed cosmological models. In Figure 5*a* we show the contour levels in the (σ_0, q_0) plane for which $P_j = 0.32$, employing models with a nonevolving burst population, photon spectral index $\alpha = 1.0$, and various limiting redshifts $z_{0.5}$. Each assumed limiting redshift produces a different region in the plane in which $P_j = 0.32$. The contour labels (1 through 4) denote the values of these limiting redshifts.

We have also indicated with a dashed line the positions of spatially flat ($k = 0$) cosmological models, which have $(3\sigma_0 - q_0 - 1) = 0$. Models with zero cosmological constant Λ are shown with the dot-dashed line. To illustrate better the regions of constant P_j, we have also truncated the x-axis at a value of $\sigma_0 = \Omega_0/2 = 0.5$, the critical density for $\Lambda = 0$. Figure 5*b* presents the same information for cosmological models in which $\alpha = 2$.

In Figures 5*c* and 5*d*, the value of P_j is lowered to 0.01 for $\alpha = 1$ and $\alpha = 2$, respectively. As expected, the contours of $P_j = 0.01$ are significantly larger than those for $P_j = 0.32$.

For a given point in the (σ_0, q_0) plane, we observe that higher limiting redshifts are required to obtain a particular value P_j for the $\alpha = 1$ spectral form than are required for $\alpha = 2$. As an example, the curve $P_j = 0.32$ found for $\alpha = 1$ and a limiting redshift of 2 (Fig. 5*a*) is similar to that found with the $\alpha = 2$ for a limiting redshift of 1 (Fig. 5*b*). Physically, because the $\alpha = 2$ spectral form is steeper, its intensity in a given energy window is more significantly affected by a given amount of cosmological redshifting. Therefore, the cosmological bending observed in the integral BATSE brightness distribution $\mathscr{N}(>P)$ is achieved at lower redshifts, and consequently the limiting redshift for bursts with $\alpha = 2$ is less than that required for $\alpha = 1$.

Figures 6*a*–6*d* present similar information to Figure 5, but for an evolutionary comoving rate density function $n_c(z) \sim (1 + z)$. The general forms of the figures are similar; however, there is one significant difference, namely, that a given value of P_j is found in the nonevolving case with lower redshifts than in the evolving case. For example, in Figure 6*a*, *no* limiting redshift below $z_{0.5} = 4$ results in a value of $P_j > 0.32$, whereas for Figure 5*a*, values of P_j larger than 0.32 can be easily found for these redshifts. Physically, this behavior is readily understood. As stronger (larger β) evolutionary forms are utilized, the brightness distribution deviates less rapidly from a Euclidean slope with increasing redshift, so that higher limiting redshifts are necessary to create a distribution consistent with the concave downward [in the log $\mathscr{N}(>P)$–log P plane) curve observed with BATSE.

Our most important result transcends all these discussions. By inspection of Figures 5 and 6, we observe the P_j contours to be strongly peaked in the lower left region of the (σ_0, q_0) plane. In addition, almost *any* cosmological model with a density in excess of the critical density ($\sigma_0 = \Omega_0/2 > 0.5$) will result in a low joint probability P_j (~ 0.01 or less), *regardless of the assumption about the burst population* (evolution, spectral index, limiting redshift, etc.). Exceptions are those rapidly accelerating ($q_0 \ll 0$) models with steep burst spectra ($\alpha \sim 2$), and limiting redshifts in excess of $z_{0.5} > 2$. The analysis is not as constraining on q_0 because for a given value of σ_0, a particular value of P_j often occurs for both positive and negative (accelerating and decelerating) values of q_0. Thus, q_0 can be said to be "restricted" to a given range, but the dynamics of models belonging to this range can be quite varied.

Therefore, we conclude that the combined measurements of H_0, τ_0, and the BATSE brightness distribution make cosmological models with the density parameter σ_0 near 0.5 ($\Omega_0 \approx 1$) or larger quantifiably less likely than low-density

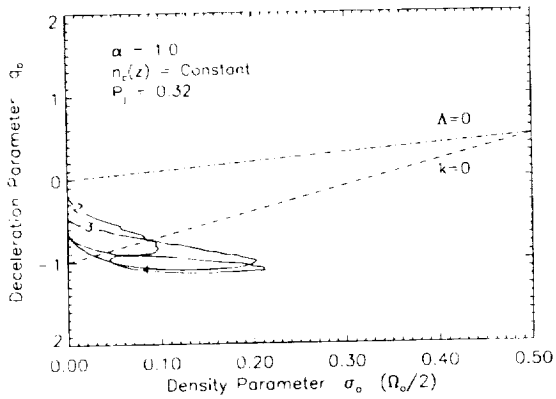

FIG. 5a

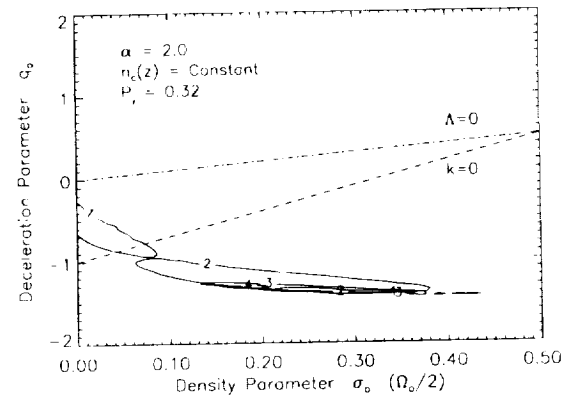

FIG. 5b

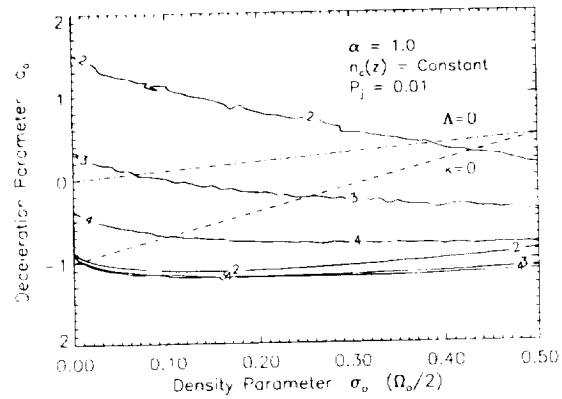

FIG. 5c

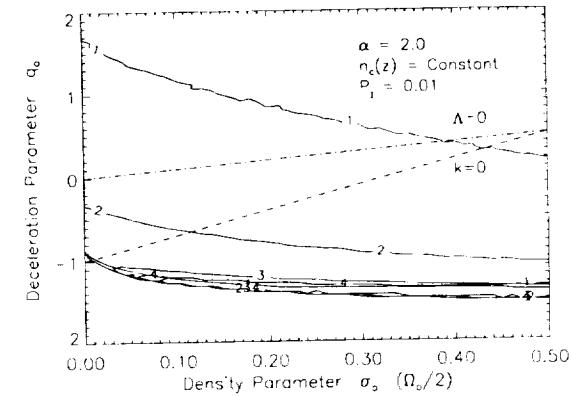

FIG. 5d

FIG. 5.—Contours of constant joint probability for nonevolving burst populations. The x-axis has been truncated at the critical density $\sigma_0 = \Omega_0/2 = 0.5$ for clarity in the contours. (*a*) Curves for $P_j = 0.32$ with a spectral index of $\alpha = 1$. The limiting redshifts used to obtain a given contour are labeled on the curves. (*b*) Similar to (*a*), but the spectral index used is $\alpha = 2$. (*c*) The value of P_j is lowered to 0.01 for the same sets of parameters used in (*a*). (*d*) $P_j = 0.01$ and $\alpha = 2$.

models based on their low P_j values, regardless of the value of q_0. The observed value of y_0 and/or the BATSE brightness distribution $N(P)$ are considerably more disparate from those that might be expected from a random sampling of these theoretical models.

5. DISCUSSION OF UNCERTAINTIES AND SYSTEMATICS

It is unlikely that the peak photon luminosities of bursts are the same for each event everywhere in the universe; however, several analyses (e.g., Emslie & Horack 1994; Hakkila et al. 1996) have shown that the range of luminosity for a significant fraction of detected cosmological bursts is indeed quite narrow (~ 10), validating the use of standard candles as a first-order assumption.

The use of a power-law spectral form for bursts is also an approximation, as burst spectra are known to exhibit evolution within a given burst and display curvature (Band et al. 1993). However, Mallozzi et al. (1996) and Horack et al. (1996a) have shown that despite their simplicity, power-law spectral forms employed in analyses of the cosmological burst brightness distribution yield quantitatively consistent answers to those obtained with more complex curved spectral forms. Further, the values of $\alpha = 1$ and $\alpha = 2$ are approximate lower and upper bounds to the spectra observed for bursts in the range 50–300 keV, and their use here is intended to bracket approximately the behavior over the range of consistent spectral models.

One may also use any number of measurements for the age of the universe or the Hubble constant. As this is an investigation into the implications of a high value for H_0, we must necessarily use measurements in the range of 70–80 km s^{-1} Mpc^{-1}, as they are commensurate with the goals of the paper. However, even within this range there are a wide variety of results that could possibly be utilized, each with their own advantages and drawbacks. We have chosen to focus on recent estimates of the age of the universe in conjunction with recent measurements of H_0 obtained from *HST* examination of the Virgo Cluster galaxy M100. We have explored the effects of utilizing different H_0 measurements than those cited here. The use of any other particular compatible H_0 measurement in place of those employed here will obviously change the computed value of y in equation (2) slightly; however, this does not alter substantially the general conclusions of the paper.

If we employ a value for H_0 that is at the low end of our set of values, for example, the $H_0 = 69$ km s^{-1} Mpc^{-1} measurement of Tanvir et al. (1995) and a value $\tau_0 = 13.5$ Gyr (a lower bound to the measurement of Bolte & Hogan 1995), one still obtains a value of $y = \tau_0 H_0 \approx 1$. This forces strong consideration of $\Lambda > 0$ models and virtually eliminates flat models with a high density parameter, including the Einstein–de Sitter model.

Depending on the assumptions one makes, the shapes of the various contours of confidence presented in Figures 4, 5, and 6 will also change. Their shapes and level values depend strongly on the magnitude of the uncertainty for y_0. Indeed, this was one impetus for utilization of the complete covariance matrix computation earlier. Future efforts to reduce

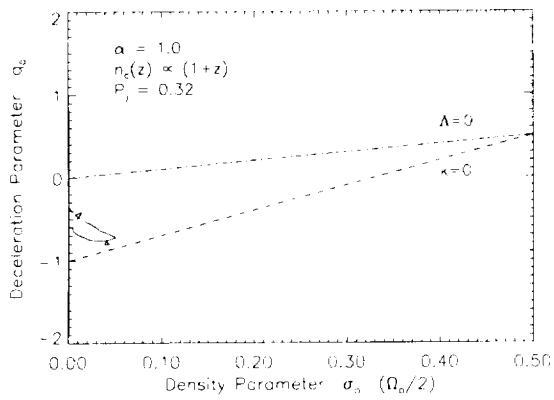

FIG. 6a

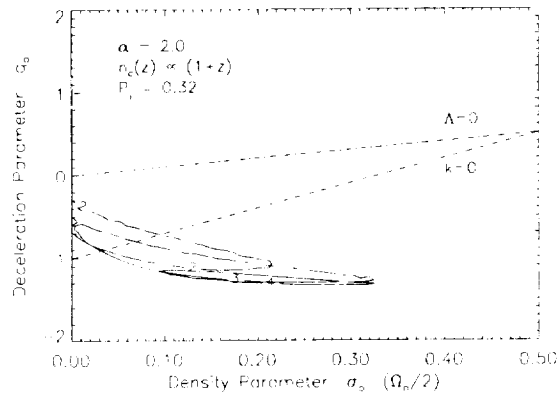

FIG. 6b

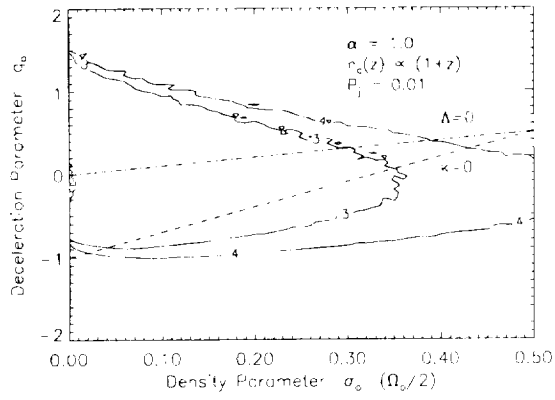

FIG. 6c

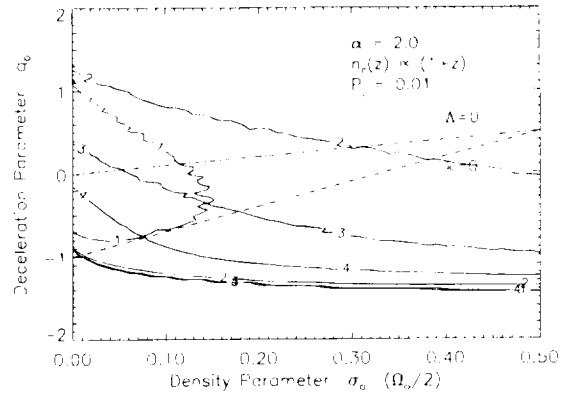

FIG. 6d

FIG. 6.—Similar to Fig. 5, but these data are produced using an evolutionary form $n_c(z) \sim (1 + z)$ for the burst comoving rate density. (*a*) No models (σ_0, q_0) employing $\alpha = 1$ result in a P_j greater than or equal to 0.32, regardless of the limiting redshifts investigated. (*b*) Contours of $P_j = 0.32$, for a spectral index of $\alpha = 2$. (*c*, *d*) The value of P_j is lowered to 0.01, and the spectral indices used in these evolving models are as shown.

the error on the measured value of H_0 to $\sim 10\%$ via the *HST* key project (see Mould et al. 1995) will further restrict nonrejectable models in the (σ_0, q_0) plane.

We have noted that the brightness distribution of bursts is not sufficiently sensitive to differentiate between $\Lambda = 0$ models, or models in which q_0 is positive (decelerating). An example of this feature was noted in the discussion of Figure 3, where $P(>\chi^2)$ is in excess of 0.5 for each decelerating model in question. Since for many "standard" cosmologies the problem is overdetermined, very large values of $P(>\chi^2)$ are not uncommon.

This is one reason for the use of the joint probability P_j rather than a different test such as the global χ^2. Indeed, when the reduced χ^2 value for the model $N(P)$ is significantly less than unity, as is the case for many of the aforementioned standard cosmologies, the further incorporation of a significant deviation in y, treated on equal footing with each individual bin of the $N(P)$ distribution, is not enough to raise the global χ^2 value significantly to a point at which the model would be rejected on the basis of this statistical test. Therefore, we have chosen the more powerful test P_j for rejection of models in the test of the null hypothesis.

That the BATSE $N(P)$ distribution and values of y can be combined in this manner to significantly restrict allowable values of (σ_0, q_0) is somewhat fortuitous. If y were measured to be significantly less than unity, the brightness distribution could not be used to further distinguish among possible cosmological models. However, with y in excess of unity, we are in a region in which small changes in σ_0 or q_0 require changes in other parameters to obtain model consistency (e.g., Emslie & Horack 1994). Thus, there is significant discriminatory power in this region, as the low-density, mildly accelerating models that cannot be distinguished from the high-density, rapidly accelerating models on the basis of y produce markedly different $N(P)$ distributions for a given α, $z_{0.5}$, and comoving rate density $n_c(z)$.

6. FURTHER ANALYSIS AND DISCUSSION

Because of the level of uncertainty in the data input to this analysis, it would likely not be productive to carry this analysis from one of hypothesis testing into one of parameter estimation in any great detail. However, examination of those cosmological models which reproduce *best* both the observed value of y_0 and the $N(P)$ distribution does offer an interesting revelation.

For a given rate density function $n_c(z)$, burst spectral index α, and limiting redshift $z_{0.5}$, the point in the (σ_0, q_0) plane that yields the largest joint probability value P_j can be considered the "best-fit" cosmological model for these input parameters. In Tables 2 and 3, we present the values of the maximum probability P_j(max) for various assumed spectral indices and limiting redshifts, as well as the values of the density parameter σ_0 (or $\Omega_0/2$) and deceleration parameter q_0 at which these maximum probabilities are found. Table 2 displays data assuming a nonevolving cosmological rate density function for gamma-ray bursts [i.e., $n_c(z)$ = constant], and Table 3 employs an evolutionary rate density of the form $n_c(z) \propto (1 + z)$.

We observe that for $\sigma_0 \neq 0$ (i.e., a model universe that is not totally empty), the maximum values of P_j are generally

TABLE 2

VALUES FOR $n_c(z)$ = CONSTANT

α	$z_{0.5}$	P_j(max)	σ_0	q_0
1.0.....	1.0	0.0073	0.00	0.08
	1.5	0.3096	0.00	−0.52
	2.0	0.6968	0.00	−0.52
	2.5	0.7917	0.04	−0.80
	3.0	0.7906	0.07	−0.92
	3.5	0.7894	0.09	−1.00
	4.0	0.7411	0.11	−1.04
1.5.....	1.0	0.1900	0.00	−0.52
	1.5	0.6918	0.00	−0.52
	2.0	0.7758	0.08	−0.96
	2.5	0.7880	0.15	−1.16
	3.0	0.7491	0.16	−1.20
	3.5	0.7721	0.18	−1.24
	4.0	0.6656	0.18	−1.24
2.0.....	1.0	0.5944	0.00	−0.52
	1.5	0.7500	0.11	−1.04
	2.0	0.8326	0.18	−1.24
	2.5	0.8058	0.21	−1.32
	3.0	0.8341	0.24	−1.36
	3.5	0.7846	0.24	−1.36
	4.0	0.7828	0.24	−1.36

found for σ_0 between 0.10 and 0.25, regardless of the assumed spectral index, evolutionary mode, or limiting redshift. These correspond to values of Ω_0 between 0.2 and 0.5, significantly less than the critical density $\Omega_0 = 1$. Each model also possesses a positive cosmological constant Λ that can be calculated as (e.g., McVittie 1965)

$$\Lambda = \frac{3H_0^2}{c^2}(\sigma_0 - q_0) . \tag{12}$$

Furthermore, each of these best-fit models lies in a region of parameter space in which the quantity $3\sigma_0 - q_0 - 1$ (the sign of which determines the spatial curvature k of the model) is small, in many cases very near zero.

We encourage readers not to overinterpret these data in light of the nature of the assumptions outside the present analysis that have to be made. For this very reason, we have not taken the analysis here an additional step further to perform detailed calculations of the best-fit values and uncertainties for each of the parameters α, $z_{0.5}$, evolutionary power-law index, σ_0, and q_0.

However, regardless of the detail of the assumptions, one result is clear. If we live in a universe that is older than $\sim$13.5 Gyr and possesses a Hubble constant in excess of $\sim$70 km s^{-1} Mpc^{-1}, the cosmological models that *best* reproduce *both* the brightness distribution of gamma-ray bursts *and* are most compliant with these aforementioned numbers possess low-mass density, with Ω_0 in the range 0.2–0.5, and a positive cosmological constant.

Furthermore, it is interesting to note that for most of these models the quantity $|3\sigma_0 - q_0 - 1|$ is small, nearly zero in some cases. The spatial curvature of a cosmological model ($k = -1, 0, +1$) is determined by the sign of $(3\sigma_0 - q_0 - 1)$. Specifically, one has the relationship (e.g., McVittie 1965)

$$k\left(\frac{c}{H_0 S_0}\right)^2 = 3\sigma_0 - q_0 - 1 . \tag{13}$$

For a fixed H_0, we observe that as the absolute value of $3\sigma_0 - q_0 - 1$ becomes very small, the value of the scale factor S_0 becomes very large. Hence, the radial coordinates r we can observe are always $\ll 1$ in these models, even for objects that might be seen at exceptionally large redshifts. In these models, then, objects cannot be observed at distances that are large enough $r \to 1$ such that the extent of the spatial curvature is appreciable. We refer to these as models with "small curvature," inasmuch as the "radius" of possible curvature is much greater than the extent of the observable universe.

On the basis of other gamma-ray burst evidence not incorporated quantitatively into Tables 2 and 3, there may be reason to consider further those models with large limiting redshifts as less likely than those with moderate values of $z_{0.5}$. These larger limiting redshifts generally result in the "best-fit" models occurring for larger values of σ_0 (and therefore Ω_0). The existence of a large limiting redshift requires (e.g., Horack et al. 1995) the $-3/2$ power law observed at the bright end of the log $\mathcal{N}(>P)$ versus log P curve to be a consequence of evolution and/or cosmological effects conspiring to produce a brightness distribution that looks at the bright end like a homogeneous population of sources distributed throughout Euclidean space, although in these instances those bursts would be neither homogeneous nor Euclidean. The existence of the $-3/2$ slope in the data is strengthened by the combination of BATSE data with observations of *Pioneer Venus Orbiter* (*PVO*) (Fenimore et al. 1993). In addition, searches for cosmologically induced time dilation (e.g., Norris et al. 1995) and spectral shifting (Mallozzi et al. 1996) have revealed no evidence of a signal strong enough to be attributed to bursts at redshifts of $z = 3$ or 4, finding instead that the data are consistent with limiting redshifts of the order $z \sim 2$ or less. Thus, on the basis of data not incorporated here, there may be further evidence to lessen the likelihood of the larger Ω_0 models shown in Tables 2 and 3.

A significant body of other observations (see, for example, Coles & Ellis 1994) indicates, that Ω_0 is likely to be in a range consistent with that found here. Among them, estimated abundances of ^{7}Li, ^{4}He, ^{3}He, and deuterium in the primordial universe agree with nucleosynthetic predictions

TABLE 3

VALUES FOR $n_c(z) \propto (1 + z)$

α	$z_{0.5}$	P_j(max)	σ_0	q_0
1.0.....	1.0	1.33×10^{-6}	0.00	1.48
	1.5	0.0005	0.00	0.56
	2.0	0.0117	0.00	−0.24
	2.5	0.0668	0.00	−0.36
	3.0	0.1774	0.00	−0.52
	3.5	0.3148	0.00	−0.48
	4.0	0.4342	0.00	−0.52
1.5.....	1.0	0.0010	0.00	0.08
	1.5	0.0694	0.00	−0.28
	2.0	0.3302	0.00	−0.48
	2.5	0.5569	0.00	−0.52
	3.0	0.6779	0.04	−0.80
	3.5	0.7869	0.06	−0.88
	4.0	0.7862	0.07	−0.92
2.0.....	1.0	0.0488	0.00	−0.36
	1.5	0.4594	0.00	−0.52
	2.0	0.6585	0.05	−0.84
	2.5	0.7894	0.11	−1.04
	3.0	0.8035	0.17	−1.20
	3.5	0.7821	0.18	−1.24
	4.0	0.7094	0.20	−1.28

(Walker et al. 1991) only if the baryonic component of the mass density Ω_b is in the range

$$100 < \Omega_b H_0^2 < 150 . \quad (14)$$

More recent estimates utilizing big bang nucleosynthesis and observed elemental abundances have constrained Ω_b to be less than 0.1 (Copi, Schramm, & Turner 1995). Only the postulation of a significant amount of nonbaryonic "dark matter" can result in a large value of Ω_0 given these small values of Ω_b.

Ostriker & Steinhardt (1995) also derive a range of Ω_0 consistent with that presented here through a combination of several independent observations of H_0 and the anisotropy of the cosmic microwave background.

Inflationary models of the universe (e.g., Guth 1981), popular on theoretical grounds, strongly favor zero spatial curvature ($3\sigma_0 - q_0 - 1 = 0$). The inflationary expansion produces enough energy to drive the universe toward a critical *total* energy density $2\sigma_0 + (\sigma_0 - q_0) = 1$, which includes contributions from mass density $2\sigma_0 (= \Omega_0)$ and a cosmological constant Λ ($\sim \sigma_0 - q_0$). Under the assumption of an appreciable value of Λ obtained from the measurements of H_0, the further strong preference for a spatially flat universe mandates a low value for $\sigma_0 = \Omega_0/2$.

Given that it is by no means a certainty that gamma-ray bursts *are* cosmological, the concurrence of *any* cosmological model with both the brightness distribution and values of y_0 may be treated with some degree of curiosity. On the basis of gamma-ray burst data alone, there is no reason to favor low-density, $\Lambda \neq 0$ models over high-density ones. Yet it is the $N(P)$ distribution of burst brightnesses which prevents the inclusion of rapidly accelerating, high-density models that could otherwise be invoked to explain the large value of y_0. Thus, the combination of the BATSE gamma-ray burst $N(P)$ distribution with the measured value of y has led to a restriction of the (σ_0, q_0) parameter space that is unobtainable from the measurements of H_0 and τ_0 alone.

7. CONCLUSIONS

We have presented the first meaningful constraints on the cosmological parameters σ_0 and q_0 to be derived, in part, from analyses of the BATSE gamma-ray burst brightness distribution. We find that in the context of a large Hubble constant (70–80 km s^{-1} Mpc^{-1}) and an age of the universe near 15 Gyr, cosmological models that possess a density near $\sigma_0 = \Omega_0/2 = 0.5$ or larger are quantifiably less likely representations of reality, as they fail to produce both values of $y_0 \equiv \tau_0 H_0$ and a burst brightness distribution $N(P)$ that agree with the observational data. This conclusion is independent of a wide range of assumptions regarding the burst evolutionary rate density, spectral index, or limiting redshift.

Furthermore, the peaked portions of the P_j contours, i.e., those models that reproduce most accurately both the observed $\tau_0 H_0$ value and BATSE brightness distribution, lie in a region of parameter space in which $\sigma_0 = \Omega_0/2 \approx 0.10$–$0.25$, significantly less than the $\Lambda = 0$ critical density. Members of this family of cosmological models are all low-density, accelerating models with a positive cosmological constant Λ, and minimal spatial curvature ($|3\sigma_0 - q_0 - 1|$ near zero).

Coles & Ellis (1994) summarize the observational evidence favoring a low-density universe, and Ostriker & Steinhardt (1995) have argued further on the basis of other data, that not only is Ω_0 within the range found here, but that the universe also is likely to have minimal spatial curvature and a positive cosmological constant. If recent measurements of the Hubble constant are substantially correct and our estimates of the age of the universe are fairly accurate, we find that these cosmological models also best explain jointly the observed value of y_0 and the BATSE brightness distribution.

We thank Peter Meszáros of the Pennsylvania State University, Jerry Fishman of NASA/MSFC, Jon Hakkila of Mankato State University, Ned Wright of UCLA, and our colleagues on the BATSE team for helpful and insightful comments to improve the manuscript. A. G. E. is supported by a *CGRO* Guest Investigator Grant from the Astrophysics Division of NASA.

REFERENCES

Band, D. L., et al. 1993, ApJ, 413, 281
Bolte, M., & Hogan, C. J. 1995, Nature, 376, 399
Briggs, M. S., et al. 1996, ApJ, 459, 40
Chaboyer, B. 1994, private communication cited in ApJ, 441, L55
———. 1995, ApJ, 444, L9
Coles, P., & Ellis, G. 1994, Nature, 370, 609
Copi, C., Schramm, D. N., & Turner, M. S. 1995, Science, 267, 192
Emslie, A. G., & Horack, J. M. 1994, ApJ, 435, 16
Fenimore, E. E., et al. 1993, Nature, 366, 40
Freedman, W. L., et al. 1994, Nature, 371, 757
Guth, A. H. 1991, Phys. Rev. D, 23, 347
Hakkila, J., et al. 1995, ApJ, 454, 134
———. 1996, ApJ, 462, 125
Horack, J. M., Emslie, A. G., & Hartmann, D. H. 1995, ApJ, 447, 474
Horack, J. M., et al. 1996a, in Proc. 3d Huntsville Gamma-Ray Burst Symposium (New York: AIP), in press
Horack, J. M., Mallozzi, R. S., & Koshut, T. M. 1996b, ApJ, 466, 21
Layden, A. C., et al. 1995, in preparation
Leonard, S., & Lake, K. 1995, ApJ, 441, L55
Mallozzi, R. S., et al. 1996, ApJ, in press
Mao, S., & Paczyński, B. 1992, ApJ, 388, L45
McVittie, G. C. 1965, General Relativity and Cosmology (Urbana: Univ. Illinois Press)
Meegan, C. A., et al. 1992, Nature, 355, 143
———. 1996, ApJ, in press
Meszáros, P., & Meszáros, J. 1995, ApJ, 449, 9
Mould, J., et al. 1995, ApJ, 449, 413
Norris, J. P., et al. 1995, ApJ, 439, 542
Ostriker, J. P., & Steinhardt, P. J. 1995, Nature, 377, 600
Paczyński, B. 1991, ApJ, 348, 485
Pierce, M. J., et al. 1994, Nature, 371, 385
Rutledge, R., Hui, L., & Lewin, W. 1995, MNRAS, 276, 753
Sandage, A., et al. 1996, ApJ, 460, L15
Sommer-Larsen, J. 1996, ApJ, 457, 118
Tanvir, N. R., et al. 1995, Nature, 377, 27
van den Bergh, S. 1991, in ASP Conf. Ser. 13, The Formation and Evolution of Star Clusters, ed. K. Janes (San Francisco: ASP), 183
———. 1992, Science, 258, 421
Walker, A. R. 1992, ApJ, 390, L81
Walker, T. P., et al. 1991, ApJ, 376, 51
Whitmore, B. C., et al. 1995, ApJ, 454, L73
Wickramasinghe, W. A. D. T., et al. 1993, ApJ, 411, L55